

Methane Activation on a $\text{La}_{0.6}\text{Sr}_{0.4}\text{Co}_{0.8}\text{Fe}_{0.2}\text{O}_3$ Perovskite; Catalytic and Electrocatalytic Results

C. Athanasiou¹, G. Marnellos¹, J.E. ten Elshof², P. Tsiakaras³,
H.J. M. Bouwmeester² and M. Stoukides¹

¹Aristotle University, Chemical Engineering Department and Chemical Process
Engineering Research Institute, University Box 1517, 54006 Thessaloniki, Greece

²Dept. of Chemical Technology, Univ. of Twente, P.O. Box 217, 7500AE, Enschede, The Netherlands

³University of Thessaly, School of Technological Sciences, Department of Mechanical & Industrial
Engineering, Athens Ave.-Pedion Areos, 383 34 Volos, Greece

Abstract: The catalytic and electrocatalytic behaviour of the $\text{La}_{0.6}\text{Sr}_{0.4}\text{Co}_{0.8}\text{Fe}_{0.2}\text{O}_3$ (LSCF) perovskite deposited on yttria stabilized zirconia (YSZ), was studied during the reaction of methane oxidation. Experiments were carried out at atmospheric pressure, and at temperatures between 600 and 900 °C. When, instead of cofeeding with methane in the gas phase, oxygen was electrochemically supplied as O^{2-} , considerable changes in the methane conversion and product selectivity were observed. The non-faradaic effects (NEMCA) were also studied and compared to those observed with metal catalysts.

1. Introduction

In the last 15 years, methane activation has been extensively investigated worldwide. As with most of the catalytic partial oxidation reactions, it was realized that a key in the various products selectivity is the type and state of oxygen used [1- 4].

Along these lines, solid electrolyte cells and particularly, oxygen ion (O^{2-}) conducting cells, were tested for methane oxidation in the last ten years [3, 4]. In such a cell, the catalyst is at the same time one of the electrodes and the reacting oxygen may be supplied electrochemically as O^{2-} through the solid electrolyte [3, 4]. One of the problems, however, is that many catalysts are oxides, not metals. The electrodes, on the other hand, must be good electron conductors (e. g., metals). The usual solution was to prepare an anodic electrode by mixing a metal with a metal oxide [4]. Nevertheless, when oxygen is electrochemically transferred, O^{2-} ions reach the metal-electrolyte-gas boundary of the anode. Consequently, methane can react with oxygen on the metal as well as on the oxide surface; and metals are poorly selective catalysts. Also, if the O^{2-} flux is high and the metal electrode is relatively inactive, a fraction of

the transported O^{2-} may combine to form gaseous dioxygen.

In the present communication, the catalytic oxidation of methane is studied on a $\text{La}_{0.6}\text{Sr}_{0.4}\text{Co}_{0.8}\text{Fe}_{0.2}\text{O}_3$ (LSCF) perovskite. This material is a mixed (O^{2-} and e^-) conductor [5, 6]. The reactor was a O^{2-} solid electrolyte cell and the LSCF served as one of the electrodes. Catalytic results obtained by using gaseous O_2 are compared to those obtained by using electrochemical O^{2-} .

2. Experimental Details

2.1. Preparation of the LSCF powder. The LSCF powder was prepared by the EDTA method. Nitrates of the constituent metals [$\text{Co}(\text{NO}_3)_2 \cdot 6\text{H}_2\text{O}$, $\text{Fe}(\text{NO}_3)_3 \cdot 9\text{H}_2\text{O}$, $\text{La}(\text{NO}_3)_3 \cdot 6\text{H}_2\text{O}$ and $\text{Sr}(\text{NO}_3)_2$] were separately dissolved in distilled water. The concentrations of all four solutions were determined by the EDTA method. Stoichiometric amounts of the solutions were mixed. The solution was then placed in a drying stove at 220 °C. After all water was evaporated, pyrolysis took place at 1000 °C for 18 hours (heating and cooling rate of the oven was 4°C/min). The powder obtained, was milled in acetone and, after drying, it was calcined at 925 °C in stagnant air for 12

hours. The calcination and milling procedures were repeated. After repeating the milling procedure, rods of 25mm diameter were obtained by unistatic pressing at 1.5 bar and isostatic pressing at 4000 bar. These rods were sintered in platinum-lined alumina boats at 1200-1225 °C for 24 hours in pure oxygen to densities between 93 - 99% of theoretical. Heating and cooling rates were 2 °C/min. Finally, the powder was milled in a ball mill for 3.5 hours. The mean particle size of the powder was determined in a particle size distribution analyzer (HORIBA LA-500 Laser-Diffraction Particle Size Distribution Analyzer). The median of the particle size was 2.44 μm and the specific area was about 3 m^2/cm^3 [6].

2.2. Apparatus for Catalytic and Electrocatalytic Measurements. The apparatus used for the catalytic and electrocatalytic measurements has been described in detail in previous communications [5, 7]. The analysis of reactants and products was done by on-line gas chromatography using a Hewlett Packard 5890 Series II with a thermal conductivity detector. Hydrogen and water were calculated from the elemental hydrogen and oxygen balance and the possibility of carbon formation was checked by closing the elemental carbon balance.

The cell-reactor consisted of an yttria-stabilized-zirconia (YSZ) tube (19 cm OD, 16 mm ID, 15 mm long), closed flat at one end. The cell was placed in a furnace which had a maximum operating temperature of 1200 °C and could maintain temperatures within 3 °C of setting. Constant currents or voltages were applied between the working and the counter electrodes with the help of a EG&G model 363 potentiostat-galvanostat. Currents and voltages were measured by means of Bar Graph HC-737 digital multimeters.

In order to prepare the working electrode (catalyst), the LSCF powder was mixed with ethyl glycol (50 mg in 20 ml of glycol) and the mixture was heated up until its volume was cut half down. The porous perovskite film was deposited on the inside bottom wall of the stabilized zirconia tube by applying a thin coating paste. The thickness of the LSCF film was of the order of 5 - 20 μm and its superficial area was about 2 cm^2 .

Silver was used for the preparation of the counter and reference electrodes as described in previous communications [8]. The LSCF electrode was deposited at the inside bottom of the YSZ tube. Then the polycrystalline silver films were deposited at the outer wall of the tube at opposite sides. When ready, the electrodes were dried at 120 °C for 30 minutes and then heated up to 500 °C for two hours. Finally the whole system was heated at 900 °C

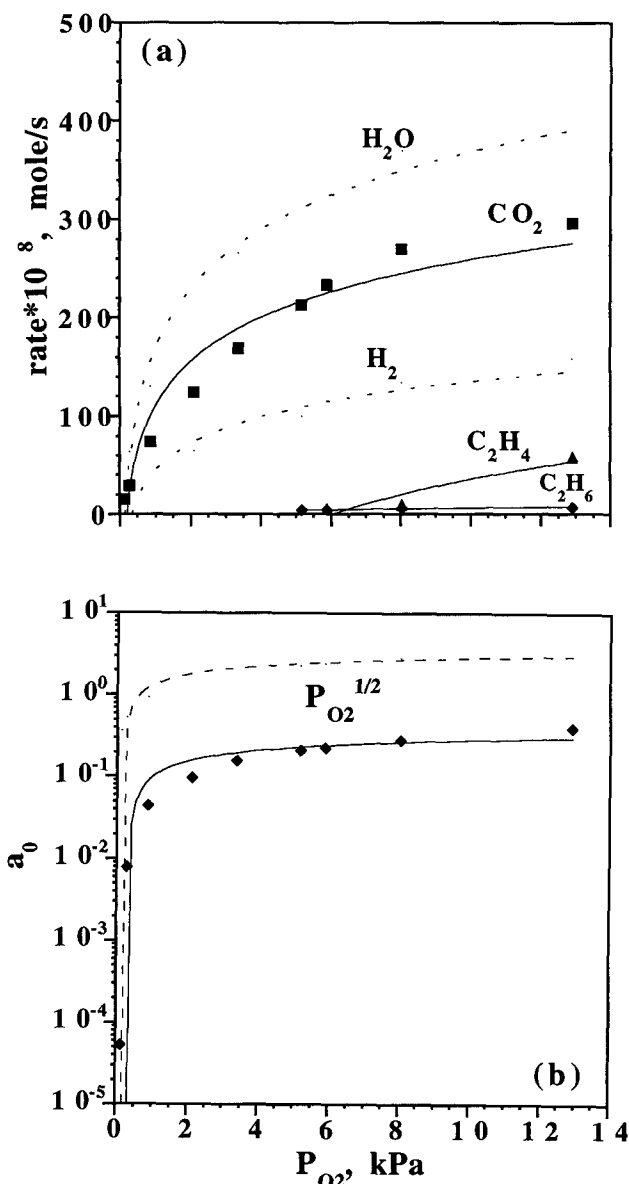


Fig. 1. Effect of P_{O_2} on the reaction rates (a), and oxygen activity (b). $T = 850\text{ }^\circ\text{C}$, $P_{\text{CH}_4} = 8\text{ kPa}$.

for 30 minutes because the catalyst had to operate at temperatures up to 880 °C. The heating rate was kept low, at about 200 °C/h.

In addition to the kinetic measurements, when operating under open-circuit, the cell-reactor can be used to obtain potentiometric data via the technique of Solid Electrolyte Potentiometry (SEP). The basic principle and applicability of SEP have been explained previously [9]. One of the electrodes of the O²⁻ cell is exposed to the reacting mixture and the other electrode is exposed to the air and serves as a reference electrode. The thermodynamic activity of atomic oxygen (a_{O}) adsorbed on the catalyst surface is given by the Nernst equation:

$$a_o = (0.21)^{1/2} \exp(2FE/RT) \quad (1)$$

where F is the Faraday constant, R is the ideal gas constant, T is the absolute temperature and E is the electromotive force of the cell. The validity of equation (1) is based on several assumptions which have been discussed in detail in previous communications [9].

3. Results

3.1. Open Circuit Measurements. The partial and complete oxidation of methane was studied in the cell-reactor at temperatures between 600 and 900 °C and atmospheric total pressure using the LSCF as an anodic electrode-catalyst. Figure 1 shows the dependence of the rates of formation of various products (1a) and of the cell potential (1b), on the oxygen partial pressure when the inlet partial pressure of methane P_{CH_4} and the temperature T were kept constant at 8 kPa and 750 °C, respectively. The dotted lines in Fig. 1a, correspond to the exit partial pressures of H_2 and H_2O as calculated indirectly via the elemental balances of hydrogen and oxygen. It can be seen that under these conditions, the major products were those of complete oxidation, i.e., CO_2 and H_2O . The rate of formation of C_2 hydrocarbons is very low and observed only at high P_{O_2} values. Figure 1b shows that for low P_{O_2} values, the oxygen activity increases drastically with increasing P_{O_2} while at higher P_{O_2} , it reaches a plateau. The dotted line above the a_o data, corresponds to the gas phase $P_{O_2}^{1/2}$ values in the reactor. If thermodynamic equilibrium were established between adsorbed and gaseous oxygen, the dotted line and the potentiometric data would coincide. Clearly, the a_o values are lower than the $P_{O_2}^{1/2}$ values.

Figure 2 shows the effect of P_{CH_4} on reaction rates (2a) and cell potential (2b) for $T=750$ °C and $P_{O_2} = 8$ kPa. Again, the rates of formation of C_2 hydrocarbons were small and the main products were still CO_2 and H_2O . The oxygen activity decreases almost linearly with P_{CH_4} .

3.2. Closed Circuit Experiments. In Figs 3a and 3b, the reaction rates are plotted vs the rate of O^{2-} transport through the solid electrolyte while the partial pressure of methane was kept at 5 kPa and 10 kPa, respectively. The O^{2-} flux is calculated from Faraday's Law and expressed in g-atoms of oxygen per second. At very low O^{2-} fluxes, the only oxygen-containing product is CO. Carbon dioxide and water start forming after a minimum O^{2-} supply is reached. The rate of CO formation reaches a maximum and then gradually goes down to zero. A carbon balance in-

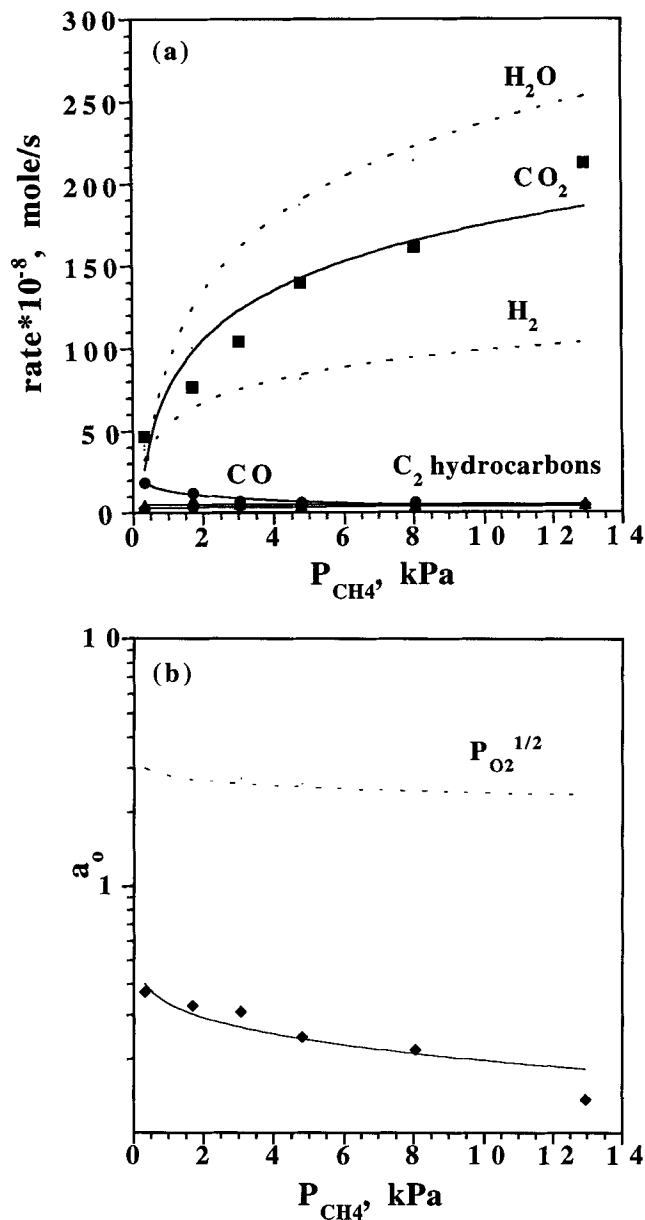


Fig. 2. Effect of P_{CH_4} on the reaction rates (a), and oxygen activity (b), $T = 850$ °C, $P_{O_2} = 8$ kPa.

dicates that carbon does form. Its formation rate seems to be unaffected by the increase in O^{2-} . This is not surprising because in these experiments, the methane to oxygen ratio was quite high. Even for the highest flux of 4×10^{-8} gatom O/s, the O_2/CH_4 feed ratio was of the order of 0.1 or less.

Figure 4 contains experimental data that were obtained under closed-circuit but in the presence of gaseous O_2 . In previous studies with such solid electrolyte cells, it has been found that under certain conditions, the increase in the rate of oxygen consumption is not equal to the rate of O^{2-} transport through the electrolyte [10]. The dimensionless rate enhancement factor Λ has been defined [10] as:

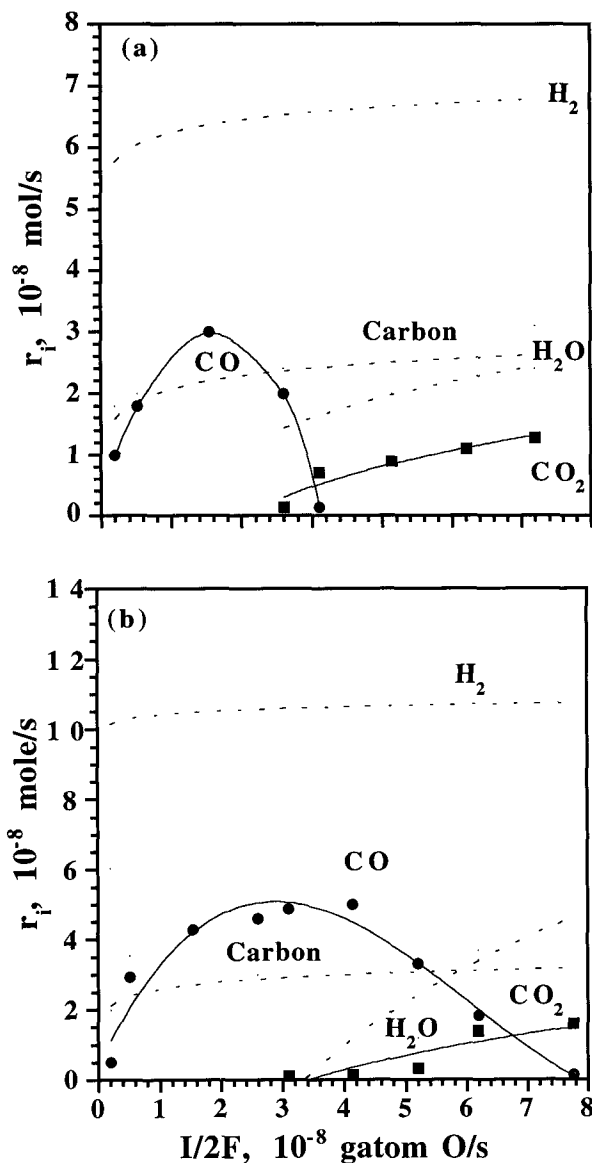


Fig. 3. Dependence of the reaction rates on the rate of the electrochemical oxygen pumping, at P_{CH_4} equal to 5 kPa (a) and 10 kPa (b).

$$\Lambda = \Delta r / (I/2F) \quad (2)$$

where Δr is the increase in the catalytic rate of oxygen consumption and $I/2F$ is the imposed flux of O^{2-} through the electrolyte [10]. In the case of a faradaic effect, all oxygen electrochemically transported through the electrolyte reacts at the anode; i.e., $\Lambda = 1$. When, for example, $\Lambda = 10^{-2}$, only 1% of the pumped oxygen reacts at the anode; the remaining oxygen combines at the anode to give molecular gaseous O_2 which can be found in the off-gas stream. Inversely, a value of Λ equal to 10^2 means that for each mole of oxygen pumped through the electrolyte, 100 moles of additional gaseous oxygen react to

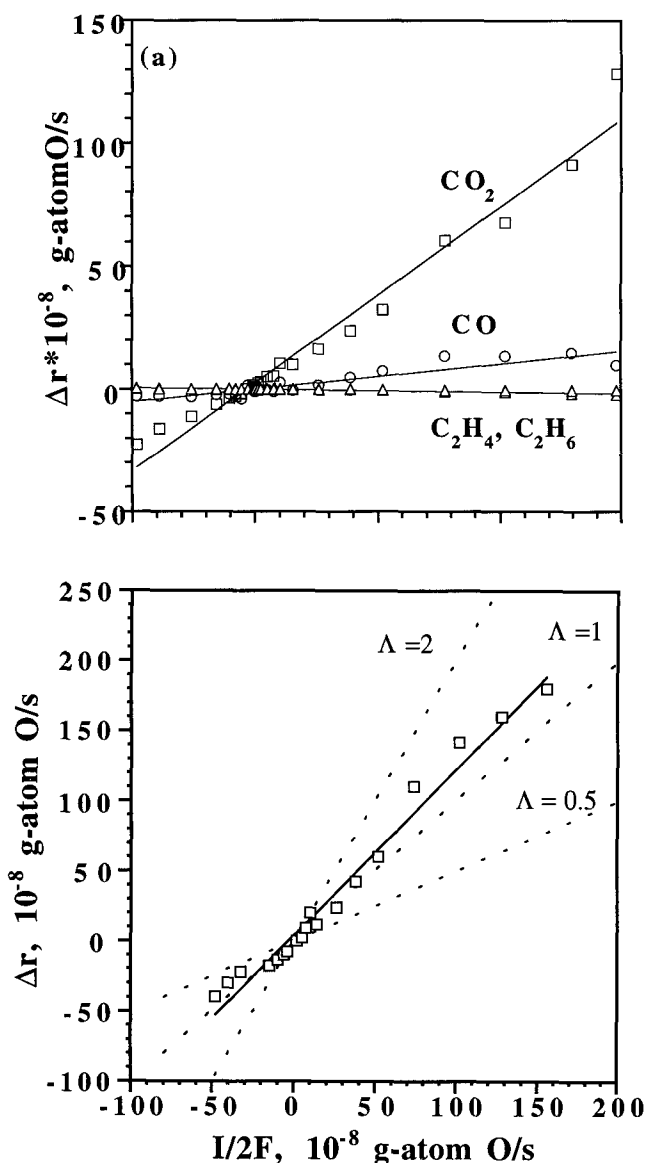


Fig. 4. Effect of electrochemical oxygen pumping on the rate of formation of various products (a) and on the total oxygen consumption (b).

form oxidation products which would not form otherwise. In this case, the presence of excess gas-phase oxygen at the anode is necessary to permit Λ to exceed unity. This phenomenon, called NEMCA, (Non-Faradaic Electrochemical Modification of Catalytic Activity), has been attributed to changes in the catalyst work function caused by oxygen pumping [10]. The data shown in Fig. 4b were obtained with a constant feed gas composition ($P_{CH_4} = P_{O_2} = 5$ kPa) and at 880 °C. The increase or the decrease in the reaction rates is plotted versus the rate of oxygen "pumping" to or from the catalyst surface. In agreement with previous works [10], current I (or equivalently, the rate of O^{2-} supply) is considered positive when oxygen is

pumped to the catalyst while it is negative when oxygen is pumped from the catalyst. Figure 4a shows that the highest rate increase is observed in the CO₂ rate, while the CO rate increases only slightly and the C₂ rates remain essentially unaffected. Negative currents have the opposite effect, i.e., all rates decrease with the CO₂ rate most affected. Figure 4b shows the Λ values attained in these experiments. Since the reaction of methane with oxygen results in a variety of products, some of which do not contain oxygen (e.g. C₂H₄ or H₂), the definition of Λ has to be modified. Hence, in the present work, Λ is based only on oxygen-containing products and is defined as:

$$\Lambda = (2 \Delta r_{\text{CO}_2} + \Delta r_{\text{CO}} + \Delta r_{\text{H}_2\text{O}}) / (I / 2F) \quad (3)$$

The values of Λ obtained are shown in Figure 4b. It can be seen that the present data fall between the straight lines that correspond to $\Lambda = 1$ and $\Lambda = 2$. This means that a non-faradaic effect is rather weak compared to other catalytic oxidations in which Λ 's as high as 10⁵ have been reported [10].

4. Discussion

The original idea of using the LSCF perovskite as a catalyst for methane oxidation was based on the two purposes that this material could serve: a) as a mixed oxide, to be a good methane coupling catalyst and b) as exhibiting good electronic conductivity, to be used as an electrode of a solid electrolyte cell. The primary goal is to focus on the different results obtained with the two types of oxygen, electrochemical (O_e) and gaseous (O_g). Hence, the present results can be summarized as follows:

- 1) The LSCF exhibits good catalytic activity towards total oxidation rather than oxidative dimerization or reforming of methane. This is a rather general observation and regardless of what oxygen source is used.
- 2) The main oxygen-containing product when O_e is used, is CO while the other oxidant produce primarily CO₂ and H₂O. Nevertheless, this distinct difference is observed at relatively low oxygen to methane ratios. At relatively high oxygen contents, (e.g. O₂/CH₄ > 1), the reaction produces total oxidation products for either type of oxygen used.

Originally proposed as good electrodes for the electrochemical reduction of oxygen [11], perovskite oxides were also found to be very effective catalysts for the complete oxidation of hydrocarbons [12, 13]. More recently, a number of perovskites have been tested as catalysts for the partial or complete oxidation of methane [2, 13, 14]. A

review of studies of adsorption and desorption of oxygen on a number of perovskites indicated that two types of oxygen, with different bonding strength, may coexist on the surface and contribute to the oxidation of methane [13]. The first type, α oxygen, is dissociatively adsorbed and accommodated in the oxygen vacancies and is more active at lower temperatures. The other type, β oxygen, is essentially lattice oxygen and its desorption is followed by partial reduction of B site cations of the perovskite. As expected, the β type oxygen is more active towards hydrocarbon oxidation at higher temperatures [13].

In the last ten years, several solid electrolyte-aided studies of methane oxidation have been reported [3, 4]. In most of these works, the solid electrolyte used was YSZ but a big variety of metal and metal-metal oxide mixtures were used as anodic electrodes. The motivation for these works was primarily based on the expected different reactivity between O²⁻ and gaseous dioxygen O₂. Actually, certain studies showed that gaseous oxygen was more selective towards C₂ products [3]. It was clear that the activity and selectivity of these cells did not depend only on the way oxygen was supplied but also on the nature of the anodic electrode.

The present results and the observed differences in catalytic activity and product selectivity with using different types of oxygen (O_e, O_g), are in agreement with findings of previous research works. Figures 1 and 2 show that O_g leads to the deep oxidation of methane. This is not very surprising if one considers that gaseous oxygen adsorbs on the LSCF and it is this loosely bound oxygen species [15] that reacts with methane.

Figure 3 shows that for low O²⁻ fluxes, the use of O_e results in the formation of CO. This can be explained by taking into account that in the absence of oxygen in the gas phase, methane pyrolysis and subsequent carbon deposition on the LSCF surface is expected to occur at these temperatures. And previous solid electrolyte aided studies reported that O_e is very effective in converting deposited carbon into CO [7, 16, 17]. A possible explanation is that the reaction occurs primarily on the surface where O_e is readily accessible.

Figure 4 indicates that a nearly Faradaic behavior is observed in the present experiments since the values of the enhancement factor Λ are very close to unity. This is not very surprising because, on one hand, the present experiments were done at temperatures 300-400 °C higher than those in which Λ values of the order of 10⁴ and 10⁵ were obtained [10]. On the other hand, in addition to surface

steps, the oxidation of methane involves non-catalytic gas-phase reactions as well [1, 2]. For these two reasons one should not expect the NEMCA effect to be significant for the present catalytic system. It should be also mentioned that the very large Λ values have been observed on metal electrodes [10]. It is possible that the NEMCA enhancement is much less pronounced when a conductive oxide and not a metal, is used as working electrode.

5. Acknowledgements

We gratefully acknowledge the financial support by the EEC under contract JOU2-CT92-0142.

6. References

- [1] E.E. Wolf, "Methane Conversion by Oxidative Processes", Van Nostrand Reinhold, New York (1992).
- [2] Y. Amenomiya, V.I. Birss, M. Goledzinowski, J. Galuszka, and A. Sanger, *Cat. Rev. - Sci. Eng.*, **3** (3), 163 (1990).
- [3] D. Eng and M. Stoukides, *Catal. Rev.-Sci. Eng.* **33**, 3759 (1991).
- [4] M. Stoukides, *J Appl. Electroch.* **25**, 899 (1995).
- [5] P. Tsiakaras, G. Marnellos, C. Athanasiou, M. Stoukides, H.J. M. Bouwmeester, J.E. ten Elshof and H. Verweij, *Sol. St. Ionics* **86-88**, 1451 (1996).
- [6] J.E. ten Elshof, H.J. M. Bouwmeester and H. Verweij, *Appl. Catal.* **130**, 195 (1995).
- [7] A. Kungolos, P. Tsiakaras and M. Stoukides, *Ionics* **1**, 214 (1995).
- [8] P.H. Chiang, D. Eng, and M. Stoukides, *Sol. St. Ionics* **67**, 917 (1994).
- [9] M. Stoukides, *Ind. Eng. Chem. Res.* **27**, 1745 (1988).
- [10] C.G. Vayenas, M.M. Jaksic, S.I. Bebelis and S. G. Neophytides, in: "*Modern Aspects in Electrochemistry*", Vol. 29, eds. J.O'M. Bockris et al, Plenum Press, New York, (1996), ch. 2.
- [11] D.B. Meadowcroft, *Nature* **226**, 847 (1970).
- [12] P.K. Gallagher, D.W. Johnson, Jr. and F. Schrey, *Mat. Res. Bull.* **9**, 1345 (1974).
- [13] T. Seiyama, *Catal. Rev.-Sci. Eng.* **34**, 281 (1992).
- [14] A.G. Andersen, T. Hayakawa, M. Shimizu, K. Suzuki and K. Takehira, *Catalysis Letters* **23**, 59 (1994).
- [15] M. Baerns and J.R.H. Ross, in: "*Perspectives in Catalysis*", eds. J.M. Thomas and K.I. Zamaraev, (Blackwell Scientific Publications 1992) 315.
- [16] H. Alqahtany, D. Eng and M. Stoukides, *Energy & Fuels* **7**, 495 (1993).
- [17] I.V. Yentekakis, Y. Jiang, S. Neophytides, S. Bebelis and C.G. Vayenas, *Ionics* **1**, 491 (1995).

Paper presented at the 4th Euroconference on Solid State Ionics, Renvyle, Galway, Ireland, Sept. 13-19, 1997

Manuscript rec. Aug. 29, 1997; rev. Sept. 15, 1997; acc. Oct. 1, 1997